Article

Effects of Cation Charge-Site Identity and Position on Electron-Transfer Dissociation of Polypeptide Cations

Yu Xia, Harsha P. Gunawardena, David E. Erickson, and Scott A. McLuckey

J. Am. Chem. Soc., **2007**, 129 (40), 12232-12243• DOI: 10.1021/ja0736764 • Publication Date (Web): 19 September 2007

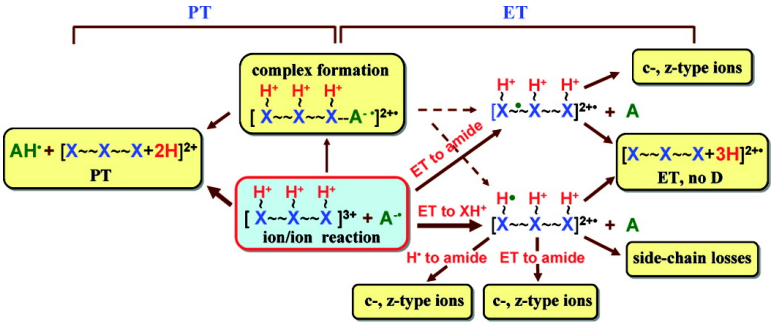

More About This Article

Additional resources and features associated with this article are available within the HTML version:

- Supporting Information
- Links to the 9 articles that cite this article, as of the time of this article download
- Access to high resolution figures
- Links to articles and content related to this article
- Copyright permission to reproduce figures and/or text from this article

View the Full Text HTML

J|A|C|S
ARTICLES
Published on Web 09/19/2007

Effects of Cation Charge-Site Identity and Position on Electron-Transfer Dissociation of Polypeptide Cations

Yu Xia, Harsha P. Gunawardena, David E. Erickson, and Scott A. McLuckey*

Contribution from the Department of Chemistry, Purdue University, West Lafayette, Indiana 47907-2084

Received May 22, 2007; E-mail: mcluckey@purdue.edu

Abstract: The effect of cation charge site on gas-phase ion/ion reactions between multiply protonated model peptides and singly charged anions has been examined. Insights are drawn from the quantitative examination of the product partitioning into competing channels, such as proton transfer (PT) versus electron transfer (ET), electron transfer followed by dissociation (ETD) versus electron transfer without dissociation (ET, no D), and fragmentation of backbone bonds versus fragmentation of side chains. Peptide cations containing protonated lysine, arginine, and histidine showed similar degrees of electron transfer, which were much higher than the peptide having fixed-charge sites, that is, trimethyl ammonium groups. Among the four types of cation charge sites, protonated histidine showed the highest degree of ET, no D, while no apparent intact electron-transfer products were observed for peptides with protonated lysine or arginine. All cation types showed side chain losses with arginine yielding the greatest fraction and lysine the smallest. The above trends were observed for each electron-transfer reagent. However, proton transfer was consistently higher with 1,3-dinitrobeznene anions, as was the fraction of side-chain losses. The partitioning of products among the various electron-transfer channels provides evidence for several of the mechanisms that have been proposed to account for electron-transfer dissociation and electron-capture dissociation. The simplest picture to account for all of the observations recognizes that several mechanisms can contribute to the observed products. Furthermore, the identity of the anionic reagent and the positions of the charge sites can affect the relative contributions of the competing mechanisms.

Introduction

The identification and structural characterization of proteins by mass spectrometry are central activities in proteome research and rely on methods of dissociation of gaseous peptide and protein ions. Structural characterization of peptide and protein ions is frequently carried out using some form of collision-induced dissociation (CID)[1] or by infrared multiphoton dissociation (IRMPD),[2] where selective fragmentation occurs at C_0-N bonds along the peptide backbone.[3] Alternatively, the interaction of thermal or near-thermal electrons with positively charged peptide/protein ions has been shown to produce fragmentation along the $N-C_\alpha$ bond thereby giving rise to a series of sequence-specific *c*- and *z*-type fragments in a process denoted as electron capture dissociation (ECD).[4−6] ECD tends to be less selective than CID in terms of the range of structurally informative channels that contribute to the product ion spectrum and, as a result, tends to provide more extensive sequence information. Also, ECD tends not to cleave bonds to post-translational modifications that are relatively labile under CID conditions.[7] Hence, ECD is a promising structural tool in proteomics. Fragmentation highly analogous to that generated via ECD has been demonstrated to result from gas-phase electron-transfer reactions to multiply protonated peptides or proteins from singly charged anions. The dissociation resulting from electron-transfer reactions has been named electron-transfer dissociation (ETD).[8,9]

The importance of ECD and ETD in peptide and protein structural characterization has motivated a number of experimental and theoretical studies designed to understand fundamental aspects related to these processes. Initial electron capture is proposed to take place into "high-lying" Rydberg states that internally convert to a "low-lying" state from which dissociation occurs.[10] An early mechanistic proposal for ECD involved electron localization at positively charged ammonium or guanidinium groups of a peptide that results in the formation of a hydrogen atom.[11] Transfer of the hydrogen atom to a nearby

(1) Wells, J. M.; McLuckey, S. A. *Methods Enzymol.* **2005**, *402*, 148−185.
(2) Little, D. P.; Speir, J. P.; Senko, M. W.; O'Connor, P. B.; McLafferty, F. W. *Anal. Chem.* **1994**, *66*, 2809−2815.
(3) Paizs, B.; Suhai, S. *Mass Spectrom. Rev.* **2005**, *24*, 508−548.
(4) Zubarev, R. A.; Kelleher, N. L.; McLafferty, F. W. *J. Am. Chem. Soc.* **1998**, *120*, 3265−3266.
(5) Zubarev, R. A.; Horn, D. M.; Fridricksson, E. K.; Kelleher, N. L.; Lewis, M. A.; Carpenter, B. A.; McLafferty, F. W. *Anal. Chem.* **2000**, *72*, 563−573.
(6) Zubarev, R. A. *Mass Spectrom. Rev.* **2003**, *22*, 57−77.
(7) Shi, S. D. H.; Hemling, M. E.; Carr, S. A.; Horn, D. M.; Lindh, I.; McLafferty, F. W. *Anal. Chem.* **2001**, *73*, 19−22.
(8) Syka, J. E. P.; Coon, J. J.; Schroeder, M. J.; Shabanowitz, J.; Hunt, D. F. *Proc. Nat. Acad. Sci. U.S.A.* **2004**, *101*, 9528−9533.
(9) Coon, J. J.; Syka, J. E. P.; Shabanowitz, J.; Hunt, D. F. *Int. J. Mass Spectrom.* **2004**, *236*, 33−42.
(10) Zubarev, R. A.; Haselmann, K. F.; Budnik, B.; Kjeldsen, F.; Jensen, F. *Eur. J. Mass Spectrom.* **2002**, *8*, 337−349.
(11) Zubarev, R. A.; Kruger, N. A.; Fridrikkson, E. K.; Lewis, M. A.; Horn, D. M.; Carpenter, B. A.; McLafferty, F. W. *J. Am. Chem. Soc.* **1999**, *121*, 2857−2862.

10.1021/ja0736764 CCC: $37.00

carbonyl oxygen of an amide groups results in cleavage of the $N-C_\alpha$ bond via an aminoketal radical intermediate.[6,10] The specificity of the dissociation is influenced by intramolecular solvation of charge (namely protons from the side chains of lysine, histidine, and arginine) by amide backbone carbonyl groups. The dissociation process was suggested to be so fast as to be nonergodic. Tureček and co-workers have since argued that, while the unimolecular rate of $N-C_\alpha$ bond dissociation is fast (10^5 s^{-1} for thermalized aminoketal radicals) on the time frame of a typical ion storage experiment (10 ms−1 s), a nonergodic hypothesis is unnecessary to account for the data.[12] Tureček and co-workers[13] and Simons and co-workers[14,15] independently proposed a "coulomb assisted dissociation model" whereby the electrostatic field associated with the excess charge of the peptide ion renders exothermic the capture of an electron into an antibonding orbital of an amide linkage. Simons et al. have since examined the likelihood for initial electron localization in a Rydberg orbital of a charge site with subsequent transfer to an antibonding amide bond orbital.[16,17] The population of such an antibonding state, either via electron capture or transfer, is posited to lead to fragmentation via conformational changes in the excited electronic state, by intramolecular proton transfer from charge sites, or by ion−dipole interactions.[15] In this mechanism, fragmentation does not necessarily require a nearby charged group to transfer mobile hydrogen atoms to the amide group of the peptide and can explain ECD experiments where characteristic *c*- and *z*-fragment ions were observed for species that lacked mobile hydrogen atoms at the charge sites.[18] Independent theoretical calculations by Uggerud et al., as well as experimental data, lend support for the possible contributions from both direct and indirect mechanisms for the origin of *c*- and *z*-fragments in ECD.[19,20] The identities of the charge bearing sites are relevant to ECD/ETD mechanisms owing to possible differences in cation recombination energies, the cation roles in determining the electronic states associated with capture, transfer, and dissociation, as well as the facility with which hydrogen atoms can be transferred to the backbone. Few experimental studies,[21,22] however, have allowed for firm conclusions to be drawn regarding the role of the positive charge bearing sites in either ECD or ETD.

In this study, focus was placed particularly on the role of cation site identity on the competition between ion/ion proton transfer and electron transfer, with or without subsequent dissociation, involving multiply protonated peptides and two reagent anions known to give rise to ETD. The results, therefore, are directly relevant to ETD but some findings may also relate to ECD as there appear to be common elements in both processes. Triply charged versions of model peptides containing different charge bearing sites, such as protonated lysine, protonated arginine, protonated histidine, or trimethyl ammonium substituents, constituted the cationic substrates. Radical anions derived from azobenzene and 1,3-dinitrobenzene were used as the electron-transfer reagents. Model peptides with mixed charge-site identities with known locations in the sequence have also been examined. These peptides reveal important insights into the initial sites of electron transfer.

Experimental Section

Materials. The peptides XGAGGXGAGGXL where all X = lysine (K), arginine (R), or histidine (H) were custom synthesized by CPC peptides (Dublin, CA). Acetic acid and acetonitrile were obtained from Mallinckrodt (Phillipsburg, NJ). Azobenzene, 1,3-dinitrobenzene, and perfluro-1,3-dimethylcyclohexane (PDCH) were purchased from Sigma-Aldrich (St. Louis, MO). The *N*-hydroxysuccinimide ester of 4-trimethylammonium butyrate (NHS-TMAB) reagent was a generous donation from Prof. Fred Regnier. The peptide fixed-charge derivatization was performed on peptide KGAGGKGAGGKL using the NHS-TMAB regent by converting the lysines and the N-terminal amine group to quaternary amines, as described in detail elsewhere.[23,24] Acetylation of the selected XGAGGXGAGGXL peptide was carried out following the standard acetylation protocol.[25] All peptides were dissolved to 10 μM in 50:49:1 (v/v/v) methanol/water/acetic acid solutions for positive nanoelectrospray ionization.

Mass Spectrometry. Experiments were performed using a commercial quadrupole/time-of-flight tandem mass spectrometer (QSTAR XL, Applied Biosystems/MDS SCIEX, Concord, ON, Canada), modified to allow for ion/ion reactions studies.[26] The major components of this tandem mass spectrometer are a quadrupole mass filter (Q1), a quadrupole collision cell that can be used as a linear ion trap for mutual ion polarity storage (Q2), and a reflectron time-of-flight (reTOF) mass analyzer for product-ion analysis. A home-built pulsed dual source[27] was coupled directly to the nanospray interface of the QSTAR instrument, comprising a nanospray emitter for the formation of positive peptide ions and an atmospheric pressure chemical ionization (APCI) needle for the formation of radical anions from the electron-transfer reagents. The experimental procedure for the electron-transfer ion/ion reactions used here has been reported in detail elsewhere.[26] In brief, a typical experiment consisted of the following steps: (1) mass-resolved anion injection into Q2 via Q1 (200 ms); (2) mass-resolved positive ion injection into Q2 via Q1 (50 ms); (3) mutual cation/anion storage in Q2 (30−50 ms); and (4) reTOF mass analysis of the positively charged ion/ion reaction products (50 ms). For each model peptide, ion/ion reactions were repeated at least three times to estimate precision, as reflected by the standard deviations in Tables 1 and 2. Peak deconvolution was performed on the charge reduced peptide ions via manual peak fitting with the assumption of Gaussian-shaped peaks.

Calculations. High level density functional theory (DFT) and *ab initio* computations using Gaussian 03[28] were carried out to obtain the structures and energies of ions and neutral species relevant to this study. Geometry optimizations, including vibrational analysis, were performed at the B3LYP/6-31+G(d) level. All stationary points were found to be true minima by carrying out vibrational frequency analysis using the

(12) Tureček, F. *J. Am. Chem. Soc.* **2003**, *125*, 5954−5963.
(13) Syrstad, E. A.; Tureček, F. *J. Am. Soc. Mass Spectrom.* **2005**, *16*, 208−224.
(14) Sobczyk, M.; Anusiewicz, W.; Berdys-Kochanska, J.; Sawicka, A.; Skurski, P.; Simons, J. *J. Phys. Chem. A* **2005**, *109*, 250−258.
(15) Anusiewicz, W.; Berdys-Kochanska, J.; Simons, J. *J. Phys. Chem. A* **2005**, *109*, 5801−5813.
(16) Anusiewicz, I.; Berdys-Kochanska, J.; Skurski, P.; Simons, J. *J. Phys. Chem. A* **2006**, *110*, 1261−1266.
(17) Sobczyk, M.; Simons, J. *J. Phys. Chem. B* **2006**, *110*, 7519−7527.
(18) Hudgins, R. R.; Hakånsson, K.; Quinn, J. P.; Hendrickson, C. L.; Marshall, A. G. Proceedings of the 50th Annual Conference on Mass Spectrometry and Allied Topics, Orlando, FL, June, 2002.
(19) Al-Khalili, A.; et al. *J. Chem. Phys.* **2004**, *121*, 5700−5708.
(20) Bakken, V.; Helgaker, T.; Uggerud, E. *Eur. J. Mass Spectrom.* **2004**, *10*, 625−638.
(21) Ivarone, A. T.; Peach, K.; Williams, E. R. *Anal. Chem.* **2004**, *76*, 2231−2238.
(22) Tsybin, Y. O.; Haselmann, K. F.; Emmett, M. R.; Hendrickson, C. L.; Marshall, A. G. *J. Am. Soc. Mass Spectrom.* **2006**, *17*, 1704−1711.
(23) Johnson, R. M.; Martin, S. A.; Biemann, K. *Int. J. Mass Spectrom. Ion Processes* **1998**, *86*, 137−154.
(24) Mirzaei, H.; Regnier, F. *Anal. Chem.* **2006**, *78*, 4175−4183.
(25) Hisada, M.; Konno, K.; Itagaki, Y.; Naoki, H.; Nakajima, T. *Rapid Commun. Mass Spectrom.* **2000**, *14*, 1828−1834.
(26) Xia, Y.; Chrisman, P. A.; Erickson, D. E.; Liu, J.; Liang, X. R.; Londry, F. A.; Yang, M. J.; McLuckey, S. A. *Anal. Chem.* **2006**, *78*, 4146−4154.
(27) Liang, X. R.; Xia, Y.; McLuckey, S. A. *Anal. Chem.* **2006**, *78*, 3208−3212.
(28) Pople, J. A.; et al. *Gaussian 03*; Gaussian, Inc.: Pittsburgh, PA, 2003.

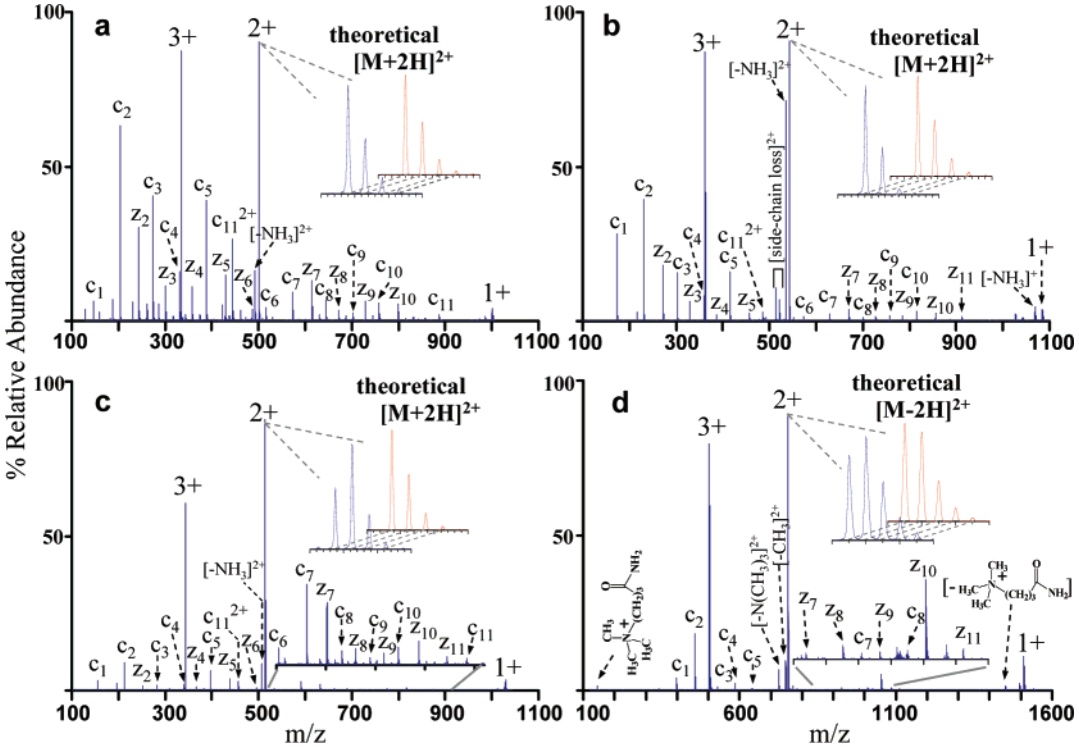

Figure 1. Post-ion/ion reaction spectra derived from reactions involving azobenzene radicals and triply charged peptide ions (a) $[M+3H]^{3+}$ of peptide K−K−K; (b) $[M+3H]^{3+}$ of peptide R−R−R; (c) $[M+3H]^{3+}$ of peptide H−H−H; and (d) $[M-H]^{3+}$ of peptide (q)t−t−t.

Table 1. Ion/Ion Reaction Product Partitioning for Various Triply Charged Peptide Cations in Reaction with the Azobenzene Radical Anions

	K–K–K	R–R–R	H–H–H	(q)t–t–t	R–R–K	R–K–R	K–R–R	Ac–R–R–R	Ac–R–R–K	Ac–K–R–R
%PT	28 ± 2	32 ± 1	34 ± 1	54 ± 2	31 ± 1	33 ± 1	24 ± 1	29 ± 2	30 ± 1	35 ± 1
%ET	72 ± 2	68 ± 1	66 ± 1	46 ± 2	69 ± 1	67 ± 1	76 ± 1	71 ± 2	70 ± 1	65 ± 1
%ETD	72 ± 2	68 ± 1	27 ± 1	25 ± 1	69 ± 1	67 ± 1	76 ± 1	71 ± 2	70 ± 1	65 ± 1
%ET, no D	<1	<1	39 ± 1	21 ± 1	<1	<1	<1	<1	<1	<1
%*c*,*z*/ETD	93 ± 1	51 ± 4	78 ± 1	67 ± 1	63 ± 1	52 ± 1	78 ± 1	51 ± 3	60 ± 1	54 ± 2
%side-chain/ETD	7 ± 1	49 ± 4	22 ± 1	33 ± 1	37 ± 1	48 ± 1	22 ± 1	49 ± 3	40 ± 1	46 ± 2

same basis set.[29,30] To determine the energies of the various species, single-point energy calculations were performed using B3LYP/aug-cc-PVTZ.

Results and Discussion

The comparison of the different charge bearing groups was carried out using a peptide sequence XGAGGXGAGGXL where X is an amino acid residue that is either a lysine (K), arginine (R), or histidine (H) group. For convenience, each peptide sequence XGAGGXGAGGXL is denoted by the symbol X−X−X, where X is substituted with the appropriate amino acid residue. The peptide (q)t−t−t is a fully derivatized analogue from peptide K−K−K, where the N-terminus and lysine primary amines are all acylated with a trimethylammonium butyrate (TMAB) group, denoted by (q) and t, respectively. Figure 1 shows product ion spectra resulting from ion/ion reactions between azobenzene radical anions and triply charged peptide cations, for example, $[M+3H]^{3+}$ of K−K−K, R−R−R, H−H−H, and $[M-H]^{3+}$ of (q)t−t−t. The insets show the isotopic distributions of 2+ product ions along with the theoretical isotope distribution of the singly deprotonated products formed via proton transfer. Note that the intact electron-transfer products should have higher masses compared to the proton-transfer products by 1 unit. It is clear from Figure 1 that proton-transfer competes with electron transfer in all cases, based on comparison of the experimental isotopic distributions of the 2+ charge states with the theoretical isotopic distributions from proton transfer. Besides the proton-transfer products, *c* and *z* ions (the latter being observed as radical ions in this study) generated via fragmentation of N−C_α bonds due to electron transfer are observed. Intact electron-transfer products are also present (i.e., $[M+3H]^{2+\bullet}$) but with varying relative contributions for different charge bearing sites. The peptide ions from H−H−H show the highest tendency of forming the intact electron-transfer products, whereas those of peptides K−K−K and R−R-R show almost no intact electron-transfer products resulting from ion/ion reactions.

The ion/ion reaction data in Figure 1 clearly show both commonalities and differences in the behaviors of the various peptide cations in reactions with the same electron-transfer reagent. To clarify the effects of the various parameters that influence the ETD process, it is instructive to account for all of the reaction channels into which products can be partitioned.

(29) Curtiss, L. A.; Raghavachari, K.; Trucks, G. W.; Pople, J. A. *J. Chem. Phys.* **1991**, *94*, 7221−7230.
(30) Foresman, J. B.; Frisch, E. *Gaussian: Exploring Chemistry with Electronic Structure Methods*, 2nd ed; Gaussian, Inc.: Pittsburgh, PA, 1996.

Table 2. Ion/Ion Reaction Product Partitioning for Various Triply Charged Peptide Cations in Reaction with the 1, 3-dinitrobenzene Radical Anions

	K–K–K	R–R–R	H–H–H	(q)t–t–t	R–R–K	R–K–R	K–R–R	Ac–R–R–R	Ac–R–R–K	Ac–K–R–R
%PT	72 ± 1	76 ± 1	78 ± 1	2 ± 1	71 ± 2	73 ± 1	74 ± 1	72 ± 1	70 ± 1	76 ± 1
%ET	28 ± 1	24 ± 1	22 ± 1	13 ± 1	29 ± 2	27 ± 1	26 ± 0.1	27 ± 1	30 ± 1	24 ± 1
%complex	<1	<1	<1	86 ± 1	<1	<1	<1	<1	<1	<1
%ETD	28 ± 1	24 ± 1	13 ± 1	5 ± 1	29 ± 2	27 ± 1	26 ± 1	27 ± 1	30 ± 1	24 ± 1
%ET, no D	<1	<1	9 ± 1	8 ± 1	<1	<1	<1	<1	<1	<1
%*c*,*z* /ETD	88 ± 0.3	37 ± 1	70 ± 1	57 ± 3	55 ± 2	38 ± 1	55 ± 1	34 ± 2	53 ± 1	40 ± 2
%side-chain/ETD	12 ± 0.3	63 ± 1	30 ± 1	43 ± 3	46 ± 2	62 ± 1	45 ± 1	65 ± 1	47 ± 1	60 ± 2

For a single ion/ion reaction involving a multiply protonated polypeptide, $[M+nH]^{n+}$, the two major competing processes are proton transfer (PT) and electron transfer (ET).[31] Essentially all proton-transfer products appear as charge-reduced peptides because subsequent fragmentation following proton transfer is rarely observed.[32] In the case of electron-transfer reactions, on the other hand, subsequent fragmentation of the charge-reduced peptide can be a significant, and often dominant, process. Hence, a full accounting of the ET channel must include both charge-reduced peptides (no apparent dissociation) and the dissociation products. Electron transfer without subsequent dissociation is referred to herein as "ET, no D". We note that a dissociation channel sometimes observed in ECD is the loss of a hydrogen atom.[33] Such a process, if it occurs in ETD, is indistinguishable from proton transfer and the products are accounted for as proton-transfer products. All other fragmentation channels can be recognized as originating from the electron-transfer reaction and they are referred to collectively as ETD products. Product partitioning percentages are determined by excluding the signal associated with unreacted precursors. Assuming no ion losses, the sum of all proton transfer (PT), electron transfer with no dissociation (ET, no D) and electron-transfer dissociation (ETD) products represents all of the precursor ions that undergo an ion/ion reaction. The percent partitioning between these three categories are therefore given in relations 1−3 respectively:

$$\%\mathrm{PT} = \frac{\sum \mathrm{PT}}{\sum \mathrm{PT} + (\mathrm{ET,noD}) + \mathrm{ETD}} \times 100 \qquad (1)$$

$$\%\mathrm{ET,noD} = \frac{\sum \mathrm{ET,noD}}{\sum \mathrm{PT} + (\mathrm{ET,noD}) + \mathrm{ETD}} \times 100 \qquad (2)$$

$$\%\mathrm{ETD} = \frac{\sum \mathrm{ETD}}{\sum \mathrm{PT} + (\mathrm{ET,noD}) + \mathrm{ETD}} \times 100 \qquad (3)$$

The total percentage of precursor ions that undergo electron transfer, %ET, is given by

$$\%\mathrm{ET} = \%\mathrm{ET,noD} + \%\mathrm{ETD} \qquad (4)$$

It is also informative to differentiate the different channels that result from ETD, for example, the *c*- and *z*-type ions due to backbone $N-C_\alpha$ cleavages and fragment ions from side-chain losses. The backbone cleavage and the side-chain losses as a percentage of total extent of ETD, referred to as %*c*,*z*/ETD and %side-chain/ETD, respectively, are defined by:

$$\%c,z/\mathrm{ETD} = \frac{\sum c,z}{\sum \mathrm{ETD}} \times 100 \qquad (5)$$

$$\%\text{side-chain/ETD} = \frac{\sum \text{side-chain}}{\sum \mathrm{ETD}} \times 100 \qquad (6)$$

The terms defined above apply to a single ion/ion reaction. In practice, contributions from sequential ion/ion reactions usually contribute to experimental data. Each sequential reaction has a distinct product partitioning. Therefore, experimental results often convolve products from different generations of ion/ion reactions. This convolution can be minimized experimentally either by the use of relatively short reaction times or some means for inhibiting sequential ion/ion reactions, such as parallel ion parking.[34] For the experiments described herein, short ion/ion reaction times (30−50 ms) were employed. The relatively large +2/+1 ratios of "intact" molecule product ions from the reactions confirm a minimal extent of two-step ion/ion reactions. Sequential ion/ion reactions, therefore, in this work are expected to give rise to inconsequential contributions to the values for %PT, %ETD, etc. Tables 1 and 2 summarize the values associated with relations 1−6 for each of the ten model cations examined in this study using the molecular anions of azobenzene and 1,3-dinitrobenzene as reagents, respectively. Reagents of relatively high electron-transfer efficiency (i.e., the azobenzene anion) and moderate electron-transfer efficiency (i.e., the 1,3-dinitrobenzene anion) were both examined to determine if consistent trends among the different cation types are noted for both types of anionic reagents. The key comparisons among the cation types are the partitioning between proton transfer and electron transfer (i.e., %PT versus %ET), the partitioning of the electron-transfer products between ETD and ET, no D (i.e., %ETD versus %ET, no D), and the partitioning among the ETD products between backbone cleavage and side-chain loss (i.e., %*c*,*z*/ETD versus %side-chain/ETD). Each of these key comparisons is addressed in turn for the K−K−K, R−R−R, H−H−H, and (q)t−t−t peptides. Results for mixed charge-site peptides are then described.

Effect of Cation Charge-Site Identity on ET versus PT. The partitioning between electron transfer and proton-transfer depends on characteristics of both the anionic reagent and the peptide cation. Proton transfer from a multiply protonated peptide to a singly charged anion is a facile process for virtually any negative ion. Electron transfer, on the other hand, competes

(31) Gunawardena, H. P.; He, M.; Chrisman, P. A.; Pitteri, S. J.; Hogan, J. M.; Hodges, B. D. M.; McLuckey, S. A. *J. Am. Chem. Soc.* **2005**, *127*, 12627−12639.
(32) McLuckey, S. A.; Stephenson, J. L., Jr. *Mass Spectrom. Rev.* **1998**, *17*, 369−407.
(33) Breuker, K.; Oh, H.-B.; Cerda, B. A.; Horn, D. M.; McLafferty, F. W. *Eur. J. Mass Spectrom.* **2002**, *8*, 177−180.
(34) Chrisman, P. A.; Pitteri, S. J.; McLuckey, S. A. *Anal. Chem.* **2006**, *78*, 310−316.

with proton transfer only when the species from which the negative ion is formed has a low electron affinity and the anion has favorable Frank−Condon factors associated with the transition from anion to neutral.[31] The characteristics of the cation that affect the partitioning among the various channels in an ion/ion reaction have not been explored systematically. Possible key variables include the absolute charge state of the cation, the degree of electrostatic repulsion in the cation (as determined by both total charge and distances between the charges within the peptide), the identities of the charge bearing sites, and the extent of intramolecular hydrogen bonding, etc. For this work, we focused on the role of the identity of the charge-bearing sites by comparing the ion/ion reaction products derived from peptide ions having the same charge states, sharing similar sequences, and reacting with the same anion reagent.

For the majority of singly charged anions, proton transfer from a multiply protonated peptide is thermodynamically favored over electron transfer to the peptide cation. This has been the case for all anions thus far observed to transfer electrons to protonated peptides. From the perspective of these gas-phase ion/ion reactions, this is significant because the distance at which the potential energies of the reactants and products are equal is greater for electron transfer than for proton transfer. In other words, the reactant and product states cross at a larger distance for electron transfer than for proton transfer and, as a result, this point is reached before the point at which proton transfer is likely. It is therefore instructive to examine the probability for electron transfer at the crossing point when considering the competition between electron transfer and proton transfer. If the probability for electron transfer is low at the crossing point, proton transfer is likely to be observed. The cross section for electron transfer (σ_{ET}) via a two-body interaction is given by

$$\sigma_{ET} = P_{ET}\pi {b_{ET}}^2 \tag{7}$$

where P_{ET} is the probability of electron transfer at classical impact parameter, b_{ET}. The square of the impact parameter for electron transfer (in atomic units) involving a multiply charged cation and a singly charged anion takes the form:[35]

$${b_{ET}}^2 = {r_{ET}}^2\left[1 + \frac{2Z_{cat}}{r_{ET}\mu {v_{rel}}^2}\right] \tag{8}$$

where Z_{cat} is the unit charge of the cation; v_{rel} is the relative velocity; μ is the reduced mass, and r_{ET} is the electron-transfer reaction distance. The latter term has been taken to be the distance at which the ground-state curves of the entrance and exit channels cross, which, for a multiply charged cation in reaction with a singly charged anion, is given (in atomic units) by

$$r_{ET} \approx \frac{(-Z_{cat})}{\Delta H_{ET}} \tag{9}$$

where ΔH_{ET} is given by

$$\Delta H_{ET} = EA(A) - RE(MH_n^{n+}) \tag{10}$$

EA(A) represents the electron affinity of reagent A, and RE(MH_n^{n+}) is the recombination energy of the cation.

The electron-transfer probability, P_{ET}, is very challenging to determine for such large systems, but a model based on Landau−Zener theory[36,37] that uses a semiempirical approximation for the coupling matrix element (see below) can provide at least a qualitative picture of the role of cation RE on the likelihood for electron transfer. The net electron-transfer probability at an avoided crossing is given by

$$P_{ET} = 2P_{LZ}(1 - P_{LZ}) \tag{11}$$

P_{LZ} is given by

$$P_{LZ} = \exp\left(-\frac{2\pi {H_{12}}^2}{\frac{dr}{dt}\left(\frac{Z_{cat}}{{r_{ET}}^2}\right)}\right) \tag{12}$$

where H_{12} is the coupling matrix element at the point of closest approach, dr/dt is the radial velocity of the reactants at the crossing point, and the remainder of the denominator gives the differences in the slopes of the entrance and exit channels at the crossing point. In the case in which one of the reactants is singly charged, the slope of the product channel at the crossing point is small relative to that of the entrance channel and is thus assumed here to be zero. The radial velocity at the crossing point can be estimated by

$$\frac{dr}{dt} \approx \left[\frac{2Z_{cat}}{r_{ET}\mu}\right]^{0.5} \tag{13}$$

The coupling matrix element, H_{12}, which indicates the strength of the electronic coupling between states, is difficult to determine *a priori* for the relatively large ions examined here. However, Olson[38,39] has presented a semiempirical relationship based on results from the study of numerous singly charged reactant pairs generated from relatively small molecules:

$$H_{12} = \left(1.044\sqrt{EA}\sqrt{RE}\left(\frac{\sqrt{2EA} + \sqrt{2RE}}{2}\right)r_{ET}\right) \times \exp\left(-0.857\left(\frac{\sqrt{EA} - \sqrt{2RE}}{2}\right)r_{ET}\right) \tag{14}$$

We have used this relationship in (12) to examine this model's predicted dependence of P_{ET} on cation recombination energy.

Figure 2 shows plots of predicted P_{ET} as a function of the cation recombination energy for the reaction of a triply charged cation with either azobenzene (blue curve) or 1,3-dinitrobenzene (red curve) radical anions. The inputs to the calculation include 300 K ions, a cation mass of 1000 Da, an anion mass of 150 Da, anion electron affinity of 0.56 eV for azobenzene, and 1.66 eV for 1,3-dintrobenzene. A maximum probability for electron transfer is found over a range of cation recombination energies. For example, the likelihood for electron transfer is optimized when the cation recombination energy is around 5.4 eV with azobenzene as the anionic reagent and higher (~7.6 eV) for 1,3-dinitrobenzene. Note that this result is relevant to ground

(35) Mahan, B. H. *Adv. Chem. Phys.* **1973**, *23*, 1−40.
(36) Zener, C. *Proc. R. Soc. London, Ser. A* **1932**, *137*, 696−702.
(37) Landau, L. D. *Phys. Z.* **1932**, *2*, 46−51.
(38) Olson, R. E. *J. Chem. Phys.* **1972**, *56*, 2979−2984.
(39) Olson, R. E.; Smith, F. T.; Bauer, E. *Appl. Opt.* **1971**, *10*, 1848−1855.

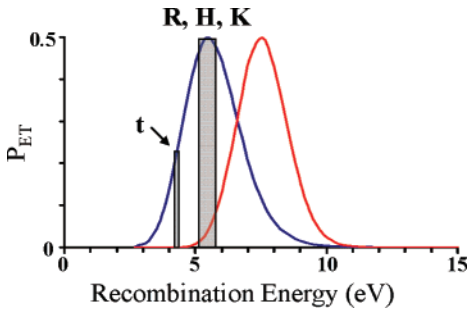

Figure 2. Electron-transfer probability versus recombination energy for the reaction of triply charged peptide cations with azobenzene (blue curve) and 1,3-dinitrobenzene anions (red curve). The gray rectangles indicate the regions where the recombination energies of different cation charge sites should fall.

state reactants and products. The decrease in P_{ET} at high values of cation RE, therefore, may not be observed experimentally if excited product states can be populated, as is likely. However, the behavior at low RE values should be expected to be observed experimentally if the model is useful.

The recombination energies for model species relevant to the different charge bearing sites examined in this work were estimated via *ab initio* calculations. For methyl ammonium, methyl guanidinium and tetramethyl ammonium, the calculated RE results are 4.2, 3.6, and 2.8 eV, respectively. These values are consistent with those reported elsewhere.[12,40] The calculated RE for protonated imidazole is reported to be 3.8 eV.[41] The presence of multiple charges of the same polarity acts to increase the intrinsic RE values of each charge site. This effect for peptides with a charge at every fifth amino acid has been estimated to be 0.8 eV for adjacent charges and 0.4 eV for one charge state removed from the nearest charge.[42] Hence, the recombination energies associated with the unmodified model peptides fall roughly in the range of 5.2−5.8 eV, which corresponds to a region of high P_{ET} for the azobenzene anion. On the other hand, the recombination energy of the TMAB modified peptide, which is estimated to be roughly 4.4 eV, falls on a region of the curve with lower P_{ET}. The experimental results in Table 1 that compare the %ET and %PT values are consistent with this model in that the %ET values are roughly similar for all of the unmodified model cations, ranging from 66 to 76%, whereas the TMAB modified species shows a %ET of 46%.

It is interesting that the species with no excess protons (i.e., (q)t−t−t) shows the highest relative proportion of ion/ion proton transfer (54%) of all of the model species. The triply charged version of this species is presumably already deprotonated at the carboxyl terminus because there are four fixed-charge sites (all three lysines and the N-terminus are derivatized). The amide hydrogens are the possible source of protons for proton-transfer reaction from the $[M-H]^{3+}$ ions. We have examined the ion/ion reaction behavior of triply charged (q)t−t−t (i.e., the $[M-H]^{3+}$ species) with perfluorinated hydrocarbon anions, such as the molecular ions derived from APCI of perfluoro-1,3-dimethylcyclohexane (PDCH), which react exclusively via proton transfer with multiply protonated peptides. The resulting product ion/ion spectra show both abundant proton transfer from (q)t−t−t cations as well as fluoride anion transfer to the cation (data not shown). Ion/ion fluoride transfer to fixed-charge derivatives of polypeptides is analogous to fluoride transfer to multiply sodiated poly(ethylene glycols), which has been noted.[43] In neither system are excess protons present. The heat of reaction for proton transfer, ΔH_{PT}, is given by

$$\Delta H_{PT} = PA(MH_{(n-1)}^{(n-1)+}) - \Delta H_{acid}(AH) \qquad (15)$$

where $PA(MH_{(n-1)}^{(n-1)+})$ represents the proton affinity of $MH_{(n-1)}^{(n-1)+}$, and $\Delta H_{acid}(AH)$ is equivalent to the proton affinity of reagent A^-. The proton affinities of the lysine, arginine, and histidine residues are about 955, 1049, and 941 kJ/mol, respectively.[44] The intrinsic proton affinity for the amide nitrogen anion is about 1514 kJ/mol.[44] The electrostatic fields of the multiply charged ion reduce proton affinities to a similar extent to which the recombination energies are increased, as discussed above. Given that similar electrostatic fields are expected to be present for all the triply charged cations, all intrinsic PA values will be decreased to a similar extent. Hence, proton transfer from the triply charged (q)t−t−t species can be expected to be significantly less exothermic than from the multiply protonated peptides. On the basis of the assumptions used above for the effect of the electrostatic field on RE values, the PA values are expected to be reduced by roughly 155 kJ/mol (1.6 eV), which places the PA of the $[M-2H]^{2+}$ ion of (q)t−t−t at roughly 1359 kJ/mol. This is a value comparable to the proton affinities of many singly charged anions. For example, the PA of the $(PDCH-F^{\bullet})^-$ anion has been estimated to be 1326 kJ/mol whereas the PA of the $(PDCH-CF_3^{\bullet})^-$ anion has been estimated to be 1456 kJ/mol.[45] The plot of Figure 2 suggests that the primary reason why proton transfer makes a greater relative contribution to the reactivity of the triply charged (q)t−t−t species than to the triply protonated peptides is largely a result of the reduced P_{ET} due to the lower RE value associated with the TMAB modified peptide. Despite the lower proton-transfer exothermicity associated with the (q)t−t−t reaction, proton-transfer yields a greater relative contribution because P_{ET} is lower for this ion.

The partitioning between proton transfer and electron-transfer clearly favors proton transfer for all of the multiply protonated species in reactions with the 1,3-dinitrobenzene anion (Table 2, rows 1 and 2), in contrast to the case for reactions with the azobenzene anion. This is consistent with Figure 2, which shows a shift in the P_{ET} curve to higher values of RE such that all of the cations are predicted to show lower probabilities for electron transfer with the 1,3-dinitrobenzene anion. Relative to one another, the protonated peptides show similar behaviors for each reagent anion. For example, the %ET associated with triply charged (q)t−t−t ions is the lowest among all the peptide ions for both anionic reagents, while the %ET values for the peptides having lysine, arginine, or histidine as charge bearing sites are similar to one another.

A unique observation was made with the reaction of (q)t−t−t with the 1,3-dinitrobenzene anion in that most of the ion/

(40) Chen, X. H.; Tureček, F. *J. Am. Chem. Soc.* **2006**, *128*, 12520−12530.
(41) Nguyen, V. Q.; Tureček, F. *J. Mass Spectrom.* **1996**, *31*, 1173−1184.
(42) Tureček, F.; Syrstad, E. A. *J. Am. Chem. Soc.* **2003**, *125*, 3353−3369.
(43) Stephenson, J. L.; McLuckey, S. A. *J. Am. Soc. Mass Spectrom.* **1998**, *9*, 957−965.
(44) NIST Chemistry WebBook, N.S.D. http://webbook.nist.gov./chemistry/ (accessed January, 2005).
(45) Newton, K. A.; He, M.; Amunugama, R.; McLuckey, S. A. *Phys. Chem. Chem. Phys.* **2004**, *6*, 2710−2717.

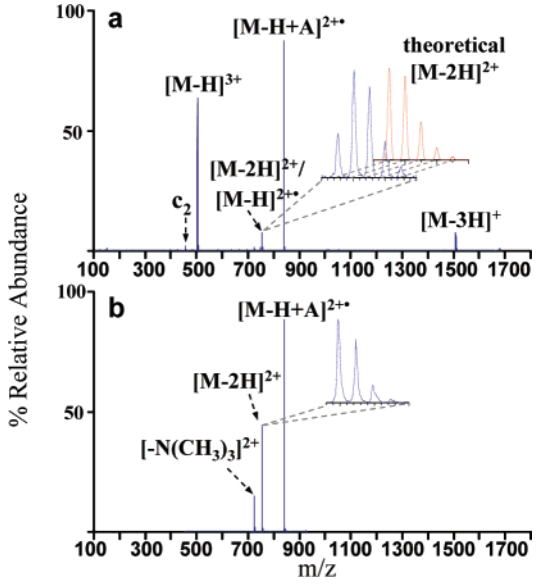

Figure 3. (a) Post-ion/ion reaction spectrum derived from reactions between 1,3-dinitrobenzene radical anions and $[M-H]^{3+}$ ions from (q)t−t−t and (b) CID spectrum of 1,3-dinitrobenzene attachment to $[M-H]^{3+}$ ions of (q)t−t−t, denoted as $[M-H+A]^{2+\bullet}$.

ion reactions between this pair resulted in the attachment of the anion to the peptide. No significant anion attachment was noted for any of the other reactant pairs, including the reaction of (q)t−t−t with the azobenzene anion (see Figure 1d). Figure 3a shows the post-ion/ion spectrum derived from reactions between 1,3-dinitrobenzene anions and the $[M-H]^{3+}$ ions from (q)t−t−t. Although some *c*- and *z*-ions as well as the charge reduced (q)t−t−t ions are present, the most dominant product ion is the adduct formed between (q)t−t−t and 1,3-dinitrobenzene, denoted as $[M-H+A]^{2+\bullet}$. Complex formation via ion/ion reactions has been observed when a large fraction of the ion/ion encounters result in a relatively long-lived collision complex and when there are significant noncovalent interactions in the complex that stabilize it with respect to fragmentation.[46,47] In the case of 1,3-dinitrobenzene anions, most of the ion/ion encounters likely involve an intimate collision because the probability for electron transfer at a crossing point, which does not require complex formation, is low (see Figure 2). Furthermore, the (q)t−t−t ions are less likely to undergo proton transfer than are the multiply protonated peptides due to lower reaction exothermicity. This lower reaction exothermicity, a stronger interaction within the complex, or a combination of both may account for the much greater tendency for attachment of the 1,3-dinitrobenzene anion than the azobenzene anion. The $[M-H+A]^{2+\bullet}$ adduct ions were isolated and subjected to collisional activation to yield the product ion spectrum shown in Figure 3b. The major CID products of $[M-H+A]^{2+\bullet}$ ions are the peptide species formed via proton transfer, $[M-2H]^{2+}$, and a product formed by subsequent loss of trimethyl amine ($[M-2H-N(CH_3)_3]^{2+}$). No product ions related to electron transfer, such as *c*,*z* ions, side-chain losses, or the intact electron-transfer products ($[M-H]^{2+\bullet}$) are observed. This result is consistent with the complex being comprised largely of the collisionally stabilized proton-transfer intermediate.

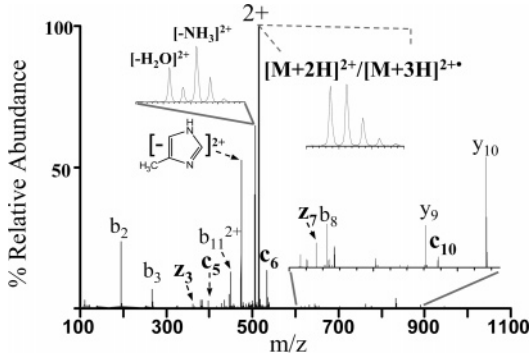

Figure 4. CID spectrum of 2+ ions derived from reaction between $[M+3H]^{3+}$ ions of H−H−H peptide and azobenzene radical anions.

Cation Effect on ETD versus ET, no D. The %ETD and %ET, no D for the peptides with different charge bearing sites are listed in Table 1, rows 3 and 4 for reactions with azobenzene anions and in Table 2, rows 4 and 5 for reactions with 1,3-dinitrobenzene. For triply charged ions from K−K−K and R−R−R, the values for %ET, no D are very small (<1%) for both reagent anions, indicating that essentially all electron-transfer products fragment before either infrared emission or collisions with background gases can stabilize the initial electron-transfer product. In the case of triply protonated ions from peptide H−H−H, the %ET, no D value is about 40% with azobenzene anions (or roughly 59% of all electron-transfer products) and roughly 9% with 1,3-dinitrobenzene anions (approximately 70% of all electron-transfer products). For triply charged (q)t−t−t, azobenzene anions gave rise to a %ET, no D value of 21% (roughly 46% of the total electron-transfer products) and reactions with 1,3-dinitrobenzene anions yielded a value of %ET, no D of 8%, which corresponded to roughly 60% of all electron-transfer products.

For a given anion, the exothermicity for electron transfer is determined by the recombination energy of the cationic species (see relation 10). If the various intact electron-transfer products have similar stabilities to fragmentation, the %ETD values might be expected to correlate with cation RE values. The recombination energies for singly charged species follow in the order lysine > histidine > arginine ≫ TMAB. The low RE of TMAB is consistent with its relatively high fraction of undissociated electron-transfer product. However, reaction exothermicity alone cannot account for the fact that H−H−H peptide cations give rise to the highest %ET, no D, as histidine has a slightly higher recombination energy than arginine. A greatly reduced extent of ECD has been reported when electron capture occurs at a cation charge site that also functions as a stable electron or hydrogen atom trap.[48] The imidazolium ion was also found to be relatively stable upon electron capture, owing to the delocalization of the nascent radical along the imidazole ring.[49] The stability of the imidazolium charge sites upon electron transfer may therefore contribute to the high fraction of %ET, no D observed for the H−H−H peptide. Figure 4 shows the results of an MS^3 experiment in which the 2+ intact peptide ions formed from reaction of the $[M+3H]^{3+}$ ion of the H−H−H peptide with azobenzene anions were isolated and subjected to collisional activation. This spectrum shows several neutral losses

(46) Wells, J. M.; Chrisman, P. A.; McLuckey, S. A. *J. Am. Chem. Soc.* **2003**, *125*, 7238−7249.
(47) He, M.; Emory, J. F.; McLuckey, S. A. *Anal. Chem.* **2005**, *77*, 3173−3182.
(48) Jones, J. W.; Sasaki, T.; Goodlett, D. R.; Tureček, F. *J. Am. Soc. Mass Spectrom.* **2007**, *18*, 432−444.
(49) Haselmann, K. F.; Budnik, B. A.; Kjeldsen, F.; Polfer, N. C.; Zubarev, R. A. *Eur. J. Mass Spectrom.* **2002**, *8*, 461−469.

as major fragmentation channels, including losses of ammonia, water, and the histidine side chain (methylimidazole, 82.053 Da). Some *c* and *z* ions are also observed together with a few *b*- and *y*-type of ions. The latter ions are likely formed from CID of the proton-transfer product ($[M+2H]^{2+}$) within the 2+ isotopic cluster. Note that no apparent loss of the methylimidazole group is observed in the reaction of $[M+3H]^{3+}$ H−H−H peptide ions with azobenzene anions (Figure 1c). The abundant histidine side-chain loss observed upon CID of the charge-reduced H−H−H ions suggests that a significant fraction of electron-transfer takes place at the histidine side chain and that the electron-transfer product is localized and stablilized on the imidazole group.

Backbone Cleavage versus Side-Chain Cleavage. The partitioning of signal among all the competing dissociation channels has direct impact on the utility of ETD for deriving primary structure information from a peptide or a protein. The partitioning of electron-transfer dissociation between informative backbone fragmentation (%*c*,*z*/ETD) and the less informative side-chain cleavages (%side-chain/ETD) for various peptides in reaction with azobenzene anions and 1,3-dinitrobenzene anions are listed in Tables 1 (rows 5 and 6) and 2 (rows 6 and 7), respectively. Substantial amounts of "side-chain" losses (49% with azobenzene and 63% with 1,3-dinitrobenzene), which can include losses of the N- or C-terminus, were observed for peptide R−R−R, including loss of ammonia and losses from arginine side-chain (loss of 44.037 and 59.048 Da).[50,51] In the cases of peptides K−K−K and H−H−H, the majority of side-chain loss is due to loss of ammonia, which accounts for 7% and 22% of the ETD products, respectively, using azobenzene anions as the reagent. As for all of the peptides in this study, somewhat greater degrees of side-chain loss were noted with 1,3-dinitrobenzene anions as the reagent. In the cases of K−K−K and H−H−H, the side-chain losses observed with 1,3-dinitrobenzene amounted to 12% and 30%, respectively. The peptide (q)t−t−t also showed abundant side-chain losses (33% with azobenzene and 43% with 1,3-dinitrobenzene). The losses observed from peptide (q)t−t−t are due to fragmentation from the TMAB group, including the loss of $\bullet CH_3$ and the loss of the fixed-charge side chain, $H_2NCO(CH2)_3N^+(CH_3)_3$. Doubly charged ions due to the loss of trimethyl amine ($N(CH_3)_3$) from the proton-transfer product were also observed, as shown in Figure 1d. Since no trimethyl amine loss was observed from proton-transfer reactions between triply charged (q)t−t−t and PDCH anions, the origin of this product is most likely due to activation of the triply charged parent ions during isolation.

The partitioning between side-chain and backbone cleavages for the multiply protonated peptides appears to be consistent with the facility for hydrogen transfer from a neutralized charge site to the peptide backbone. Hydrogen transfer is a key step in the ECD/ETD process that involves electron capture/transfer to a protonated site with subsequent hydrogen transfer to the backbone. Tureček et al. have examined this process via theoretical calculations and conclude that hydrogen transfer from a protonated amine site, such as the side chain of a protonated lysine residue, is a very facile process,[12] whereas a substantial energy barrier exists for hydrogen-atom transfer from a guanidyl radical site to an amide group.[40] For this reason, hydrogen transfer from a neutralized arginine side chain is inhibited, thereby increasing the likelihood for the observation of losses associated with the arginine side chain. The results reported here are consistent with this difference between the neutralized side chains in that the K−K−K species shows the least side-chain cleavage and the R−R−R species shows the most side-chain cleavage. In the case of histidine radical residues, internal H-atom migration is thermoneutral or only slightly exothermic and therefore might be expected to lead to a propensity for hydrogen transfer that is intermediate to the lysine and arginine cases.[52] Given that the histidine radicals are relatively stable, side-chain cleavage may be less likely than for the arginine case. The relatively large %ET, no D value for the H−H−H system may therefore reflect both a high radical stability and a moderate to low propensity for hydrogen transfer.

The results for the multiply protonated peptides provide strong evidence for the importance of hydrogen transfer from a neutralized charge site in providing high %*c*,*z*/ETD values. They do not, however, preclude the other proposed mechanisms for the formation of *c*- and *z*-type ions since all of the protonated species resulted in backbone cleavage. The peptide (q)t−t−t is relevant in this regard in that neutralization of the charge site is not expected to yield a labile hydrogen atom. The $[M-H]^{3+}$ ion derived from the (q)t−t−t has the second lowest %*c*,*z*/ETD among the four peptides, which may be a direct consequence of the lack of protons at the charge sites. However, it is also noteworthy that even in the absence of labile protons, the (q)t−t−t peptide has a higher partitioning of backbone fragments than does peptide R−R−R. This result suggests that either the direct electron capture by or transfer (either from a reagent anion or from a Rydberg state localized on a charge site) to an amide linkage can contribute to the formation of at least some *c*-and *z*-type ions.[13−15] Similarly, in the ETD of several model disulfide-linked peptides, the relative contribution from *c*- and *z*-type fragments decreased with the fixed-charge derivatives but did not disappear.[53] On the other hand, cleavage of the disulfide linkages increased in relative abundance for the fixed-charge derivatives relative to the multiply protonated analogues. This result suggested that the presence of excess protons plays a more important role in formation of *c*- and *z*-type ions than in the preferential cleavage of disulfide bonds via either ETD or ECD. The results collected here support the evidence already in hand that the presence of excess protons can facilitate amide bond cleavage in ETD and ECD, but this is not an absolute prerequisite.

A summary of the overall interpretation for the charge-site identity effects noted here for the electron-transfer pathways is facilitated with reference to the kinetic scheme of Figure 5. This scheme shows several competing pathways for the initial ion/ion reaction step as well as sequential reactions from several of the initially formed ion/ion reaction products. The diagram shows an arrow for direct proton-transfer that represents transfer at a crossing point without formation of a long-lived ion/ion reaction intermediate. Another arrow represents the formation of a long-lived complex, dissociation of which yields proton-transfer products. It is also recognized that electron-transfer

(50) Cooper, H. J.; Hudgins, R. R.; Hakånsson, K.; Marshall, A. G. *J. Am. Soc. Mass Spectrom.* **2002**, *13*, 241−249.
(51) Pitteri, S. J.; Chrisman, P. A.; McLuckey, S. A. *Anal. Chem.* **2005**, *77*, 5662−5669.
(52) Tureček, F.; Chen, X. Proceedings of the 54th ASMS Conference on Mass Spectrometry and Allied Topics, Seattle, WA, May, 2006.
(53) Gunawardena, H. P.; Gorenstein, L.; Erickson, D. E.; Xia, Y.; McLuckey, S. A. *Int. J. Mass Spectrom.* **2007**, *265*, 130−138.

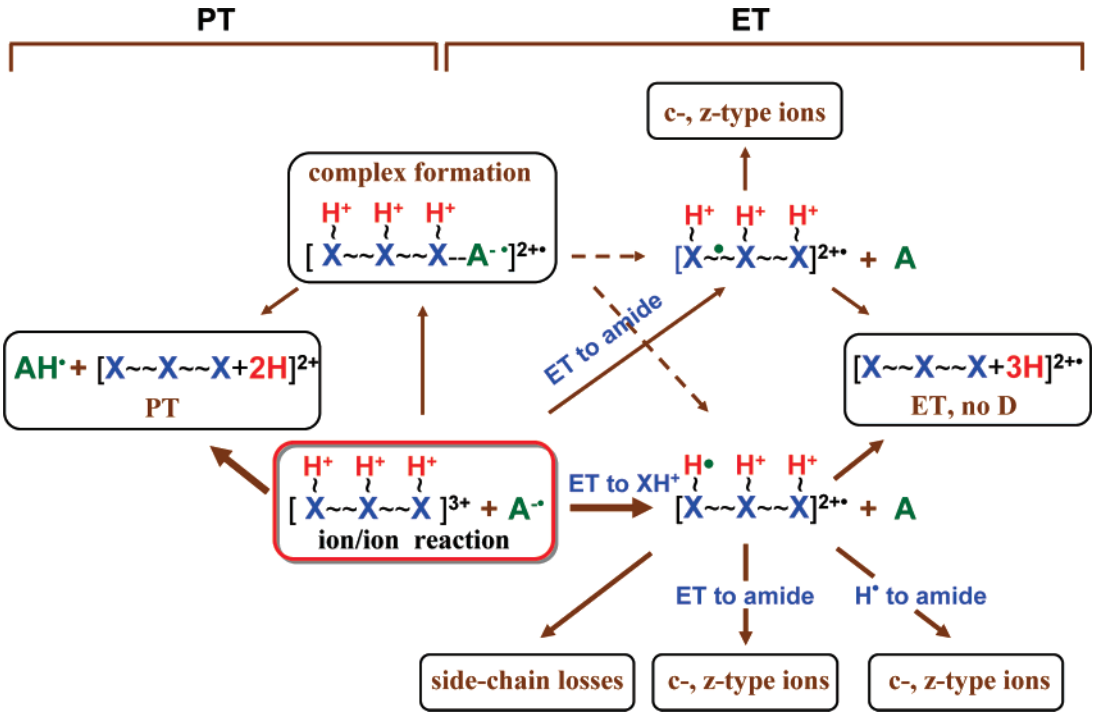

Figure 5. Kinetic scheme for the ion/ion reactions between triply charged model peptides with a reagent anion, $A^{-\bullet}$.

products can be formed via a complex but no clear evidence for this pathway has been noted in this work. Therefore, dashed arrows are used in the diagram of Figure 5 to indicate this possibility. Two distinct arrows are used to represent direct electron transfer at a crossing point. One indicates direct transfer to an amide bond, which represents the mechanism forwarded by Tureček and Simons. A rapid cleavage to yield *c*- and *z*-type ions is assumed to result from this pathway. The other indicated electron-transfer pathway represents electron transfer to a charge site. From this product, dissociation of the neutralized side chain, transfer of a hydrogen atom to an amide bond, and transfer of an electron from a Rydberg state populated by electron transfer to a charge site to an amide bond are indicated as the main subsequent events. Both the hydrogen-transfer mechanism and the electron-transfer mechanism, which Simons has referred to as through-bond intramolecular electron transfer,[54] lead to *c*- and *z*-type ions. A fourth possible outcome from the electron transfer to a charge site is stabilization of the ion either via collisions or emission to lead to the observation of the undissociated electron-transfer product (i.e., ET, no D).

For the triply charged model species studied here, the electrostatic fields associated with the cations are expected to be comparable such that similar probabilities for a direct electron transfer from a given reagent to an amide bond are expected. Comparison of the data collected with the different reagent anions provides the most compelling evidence for a contribution from this pathway. The %side-chain/ETD values resulting from reactions with 1,3-dinitrobenzene anions are consistently higher than they are from reactions with the azobenzene anions. This is most readily rationalized on the basis of the higher electron affinity of 1,3-dinitrobenzene. The likelihood for electron transfer to an amide linkage, the electron affinity of which is much lower than that of the charge site, is expected to be lower as the EA of the reagent increases. This results a higher fraction of electron transfer to the charge site and, hence, a higher relative contribution from side-chain cleavage.

The other major trends observed in the data are more readily accounted for on the basis of electron transfer to a charge site and the subsequent reaction channels associated with this pathway. Hydrogen transfer from lysine to an amide linkage is a facile and apparently fast process, which results in a minimal degree of side-chain cleavage. Hydrogen transfer is less facile from either arginine or histidine, which inhibits the hydrogen-transfer channel for the formation of *c*- and *z*-type ions. Side-chain losses from arginine are relatively facile, which results in the highest degree of side-chain loss among the three basic amino acids. Histidine, on the other hand, forms relatively stable radicals with relatively long life-times with respect to either fragmentation or hydrogen transfer. As a result, ET, no D is most prominent with the H−H−H species.

The Effect of Lysine Residue Position on Electron-Transfer Dissociation. The effect of lysine residue position on electron-transfer dissociation behavior was evaluated for peptides K−R−R, R−K−R, R−R−K, and N-terminally acetylated versions of R−R−R, K−R−R, and R−R−K, denoted as Ac−R−R−R, Ac−K−R−R, and Ac−R−R−K, respectively. The partitioning of products formed from reactions with azobenzene anions is summarized in Table 1, and the results from reactions with 1,3-dinitrobenzene anions are listed in Table 2. In terms of the competition between proton transfer and electron transfer, the position of the lysine residue appears to show no dramatic effect for either of the anions. As with the other model peptides, 1,3-dinitrobenzene anions lead to a significantly greater extent of proton transfer for all of the ions. Essentially no ET, no D products (<1%) were detected, which is consistent with the strong ETD tendencies observed for the K−K−K and R−R−R ions. Hence, for a given reagent anion, the %ETD values are similar. Figure 6 summarizes the relative abundances of *c*- and *z*-type ions as a function of peptide

(54) Sobczyk, M.; Simons, J. *Int. J. Mass Spectrom.* **2006**, *253*, 274−280.

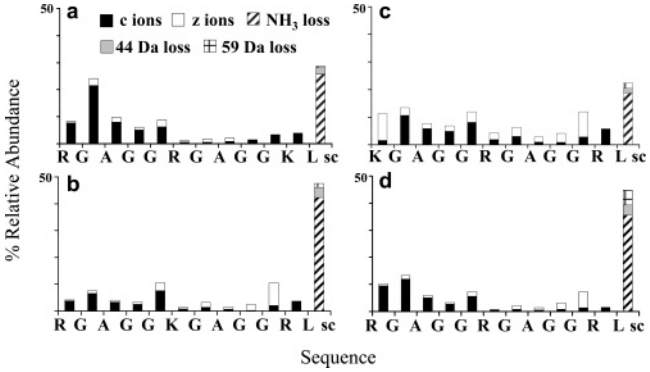

Figure 6. Relative abundances of product ions resulting from reaction of azobenzene anions with $[M+3H]^{3+}$ ions from (a) R−R−K, (b) R−K−R, (c) K−R−R, and (d) R−R−R; "sc" represents observed side-chain losses.

sequence together with an entry for the side-chain losses, resulting from reaction between azobenzene anions and $[M+3H]^{3+}$ ions from R−R−K, R−K−R, K−R−R, and R−R−R. The contributions to the total side-chain loss signal due to ammonia loss and the losses of 44 and 59 Da from the arginine side-chain are also indicated. The relative abundance for each fragment ion was acquired by normalizing to the total abundance of the ETD products.

For peptides R−R−K, R−K−R, K−R−R, and R−R−R, three of the most prominent backbone fragment channels are between residues Gly^2-Ala, Gly^5-Xxx and Gly^{10}-Xxx (Xxx = Lys, Arg). Since the charge-bearing sites for each triply protonated peptide are most likely to be located at the basic residues, which are at sequence positions 1, 6, and 11, the observed fragmentation channels indicate a promotion of backbone $N-C_\alpha$ cleavage near the charge-bearing sites. Similar tendencies are also observed for peptides X−X−X (X═K, H, or R). However, the tendency is subtle and evidence for all other possible amide bond cleavages is present for all of the peptide ions examined. There is no strong correlation between the relative contributions of the various backbone-cleavage channels and the position of the lysine residue.

The position of the lysine residue in the sequence, however, appears to play an important role in determining the partitioning between backbone cleavages and side-chain losses. The %side-chain/ETD values for K−R−R, R−K−R, and R−R−K in the azobenzene data set (see Table 1) are 22%, 48%, and 37%, respectively. For comparison, the value for K−K−K was determined to be 7% and that for R−R−R was found to be 49%. On the basis of these values, the R−K−R ion behaves much like the R−R−R ion, whereas the K−R−R and R−R−K ions show behavior that is intermediate between R−R−R and K−K−K, with K−R−R showing the least side-chain loss of the three mixed-charge site peptides. Side-chain losses from charge sites are associated with electron transfer to the charge site (see Figure 5). The observation that the extent of side-chain loss is a function of the position of the lysine residue implies that the likelihood for electron transfer to the lysine is affected by its position in the peptide. An interpretation for this effect is illustrated in Figure 7. The top of the figure shows a segment of the energy diagram for a reaction between a multiply protonated peptide and a singly charged anion. The entrance channel follows an attractive $^1/_r$ dependence, while a very weak attraction is expected for the ion/neutral surface associated with the products. Exit channels for "high" and "low" reaction

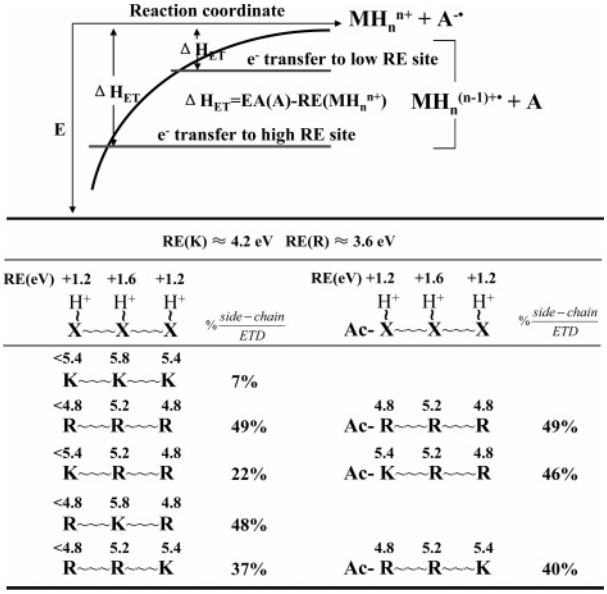

Figure 7. Hypothetical potential energy curves for an ion/ion reaction involving electron transfer from a singly charged anionic reagent $A^{-\bullet}$ to a protonated lysine or arginine residue of a multiply protonated peptide or protein MH_n^{n+}, as well as estimated RE values for various sites in the indicated model peptides.

exothermicity cases are indicated. The impact parameters for electron transfer at the crossing points are inversely related to the respective reaction exothermicities (i.e., the crossing point for the lower reaction exothermicity reaction occurs at a larger distance (see relation 9). Provided the P_{ET} values are comparable (see relation 7), the cross-section for the site with the lower RE value will be larger than the site with the higher RE value. Note that this picture represents an instance in which the kinetically favored product site (i.e., one with a low RE) differs from the thermodynamically favored site. Figure 7 also provides a tabular summary of RE values of the charge sites within each peptide based on estimates made elsewhere in this work (i.e., intrinsic RE of lysine = 4.2 eV, intrinsic RE of arginine = 3.6 eV, the increase in RE value for central charge site = 1.6 eV, and the increase in RE value for a charge at either the N- or C-terminus of the peptide = 1.2 eV). The RE value of the residue at the N-terminus is expected to be lower than the estimated value of the side chain due to the stabilization of charge by interaction with the N-terminal amino group (i.e., the RE of a protonated site is inversely related to the proton affinity of an unprotonated site). For this reason, the estimated RE value is listed as an upper limit. Data were also collected for R−R−R, K−R−R, and R−R−K after a single acetylation. In the cases of R−R−R and R−R−K, the N-terminus is acetylated, whereas in the case of K−R−R, either the N-terminus or the lysine amino group is acetylated. (The *c*-and *z*-ions formed from Ac−R−R−K indicated essentially no acetylation at the C-terminal lysine.) Nevertheless, for the Ac−K−R−R case, acetylation at either site is expected to increase the RE value of the N-terminal amino acid.

The peptide ion with the lowest %side-chain/ETD value, that is, K−R−R, is also the species in which electron transfer to the lysine side chain is most probable (i.e., where the RE value for lysine is lowest due to both the presence of the amino terminus and the fact that the site is one of the two that experiences the lowest electrostatic field). In the case of R−K−

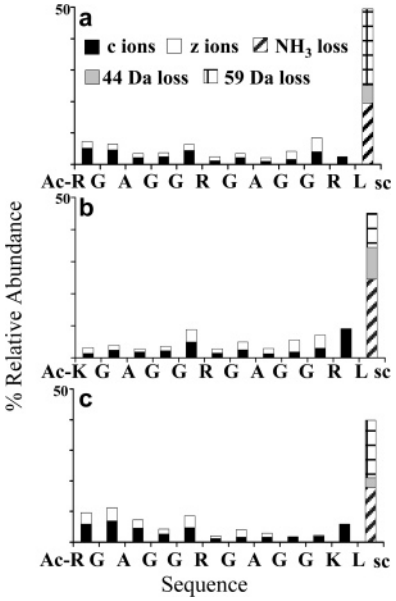

Figure 8. Summary of ETD results for reactions of azobenzene anions with (a) Ac−R−R−R, (b) Ac−K−R−R, and (c) Ac−R−R−K.

R, the lysine is in a position with the highest RE value because of the absence of a nearby stabilizing amino terminus and the presence of the highest electrostatic field. This species shows almost as much side-chain loss as R−R−R, which suggests that electron attachment at the lysine in this peptide is relatively small. When K−R−R is acetylated, the %side-chain/ETD value increases from 22% to 46%, suggesting that attachment at the lysine residue has been significantly reduced by eliminating the adjacent amino terminus. Acetylation of R−R−K has little effect on %side-chain/ETD. Qualitatitively similar observations are noted with the data collected using 1,3-dinitrobenzene anions. That is, R−K−R yields a %side-chain/ETD value similar to that for R−R−R, while those from K−R−R and R−R−K yield lower %side-chain/ETD values. Upon acetylation, Ac−K−R−R yields a %side-chain/ETD value similar to that of R−R−R while Ac−R−R−K shows little change in %side-chain/ETD.

The relative abundances of the specific side-chain products are also consistent with favored electron attachment at sites with the lower RE values. All of the unmodified peptides show loss of ammonia to be the dominant side-chain fragmentation. However, loss of the amino terminus can contribute to this signal such that the side-chain losses from R−R−R, for example, can include ammonia loss associated with the N-terminus. The results for Ac−R−R−R, therefore, provide a better picture of the inherent behavior of the arginine side chain. Figure 8 shows summaries of the ETD results for Ac−R−R−R, Ac−K−R−R, and Ac−R−R−K. (Note that methyl esterification of the C-terminus has no effect on the product partitioning (data not shown)). The acetylated version of R−R−R yields the same %side-chain/ETD value as unmodified R−R−R but the side-chain losses are significantly shifted toward a loss of 59 Da (compare Figure 6d with Figure 8a). Acetylation of the N-terminus of K−R−R leads not only to an increased %side-chain/ETD value but also significantly greater loss of 59 Da (compare Figure 6c with Figure 8b). This observation is also consistent with the interpretation that more of the electron-transfer events take place at the arginine residues after acetylation.

Within the context of the scheme of Figure 5, the identity of the amino acid charge bearing site is expected to play little role in the direct electron transfer to an amide bond because this probability is governed largely by the electrostatic field. For the model peptides in this work, the electrostatic field is not expected to be a significant variable. Hence, the position of the lysine residue is not expected to significantly affect the pathway to *c*- and *z*-type ions that proceeds via direct electron transfer to an amide linkage. The role that the lysine position plays derives from the pathways that proceed via electron transfer to a charge site. The position of a basic residue within a multiply charged peptide can have a major effect on its RE value which, in turn, plays a significant role in determining the likelihood of electron transfer to the site. Interestingly, the results collected here suggest that electron transfer to the thermodynamically favored site, which would be the lysine in triply protonated R−K−R, is disfavored. Rather, kinetically favored sites appear to be preferentially populated. It is noteworthy that this observation is dependent upon the relatively rapid side-chain loss channel of arginine. If side-chain loss were slow relative to intramolecular electron transfer between charge sites, the R−K−R ion would be expected to show relatively little side-chain loss and the kinetic effect would be obscured.

Conclusions

Four types of cation charge-bearing sites, for example, protonated lysine, arginine, histidine, and trimethyl ammonium were evaluated for electron-transfer ion/ion reactions involving triply charged model peptide cations and radical anions derived from azobenzene or 1,3-dintrobenzene. Quantitative measures of product ion partitioning between competing channels, such as proton transfer versus electron transfer (%PT versus %ET), electron transfer with and without subsequent dissociation (%ET, no D versus %ETD), and the competition between backbone and side-chain cleavages (%*c*,*z*/ETD versus %side-chain/ETD), enable insights to be drawn regarding key elements in the ETD process. For the peptide cations studied herein, the probability for electron transfer follows the order: (lysine ≈ histidine ≈ arginine) > trimethyl ammonium. The experimental results correlate with the trend of electron-transfer probability predicted by a model based on Landau−Zener theory. The model can account for the comparable %ET values for the three unmodified peptides and the lower %ET values obtained for the TMAB modified peptide. It also can account for the generally lower %ET values observed with 1,3-dinitrobenzene anions.

A significant yield of *c*-and *z*-type ions from the TMAB derivatized peptide with no excess protons suggests that mechanisms that do not require the initial generation of a hydrogen atom can contribute to ETD data. These include direct electron transfer to an excited-state of an amide linkage and the transfer of an electron from a Rydberg orbital of a charge site to an amide linkage. The higher extents of side-chain cleavage with the higher EA reagent 1,3-dinitrobenzene is most readily accounted for by a reduction of the likelihood for direct electron transfer to an amide bond. However, several trends in the data are most readily interpreted on the basis of initial electron transfer to a charge site with a subsequent competition between side-chain cleavage, hydrogen transfer to a nearby carbonyl group with subsequent amide bond cleavage, or electron transfer to a nearby amide bond with subsequent bond cleavage. The high %ET, no D values noted for histidine, the

high propensity for side-chain losses from arginine, and the low propensity for side-chain losses from lysine are most readily interpreted on the basis of initial electron localization at the charge site. The relative stability of histidine radicals to either fragmentation or hydrogen transfer lead to the observation of significant quantities of intact electron-transfer products. The relative lability of the arginine side-chain and its low propensity for hydrogen transfer lead to a high degree of side-chain cleavage. The facility with which hydrogen can transfer from lysine to an amide linkage, on the other hand, can account for the low extent of side-chain loss as well as the lack of intact electron-transfer survivors. The mixed charge site studies provide evidence for initial electron transfer to and side-chain cleavage from kinetically favored sites. Overall, these studies provide evidence for contributions from competing ETD mechanisms. Factors identified that can affect the partitioning between competing pathways include cation recombination energy, the electron affinity associated with the anionic reagent, the propensities for neutralized charge sites to fragment, yielding side-chain losses, or to transfer a hydrogen (or an electron) to an amide linkage.

Acknowledgment. The authors acknowledge support from the office of Basic Energy Sciences, Division of Chemical Sciences under Award No. DE-FG02-00ER15105 and the National Institutes of Health under Grant GM 45372.

Supporting Information Available: Full citations for refs 19 and 27. This material is available free of charge via the Internet at http://pubs.acs.org.

JA0736764